Hydrol. Earth Syst. Sci. Discuss., 10, 12905–12950, 2013
www.hydrol-earth-syst-sci-discuss.net/10/12905/2013/
doi:10.5194/hessd-10-12905-2013

Hydrology and Earth System Sciences
Open Access
Discussions

Validating a spatially distributed hydrological model with soil morphology data

T. Doppler[1,2], M. Honti[1], U. Zihlmann[3], P. Weisskopf[3], and C. Stamm[1]

[1]Swiss Federal Institute of Aquatic Science and Technology (Eawag), Dübendorf, Switzerland
[2]Swiss Federal Institute of Technology (ETH), Zürich, Switzerland
[3]Agroscope Reckenholz-Tänikon, Zürich, Switzerland

Received: 13 August 2013 – Accepted: 14 October 2013 – Published: 30 October 2013

Correspondence to: C. Stamm (christian.stamm@eawag.ch)

Published by Copernicus Publications on behalf of the European Geosciences Union.

Abstract

Spatially distributed hydrological models are popular tools in hydrology and they are claimed to be useful to support management decisions. Despite the high spatial resolution of the computed variables, calibration and validation is often carried out only on discharge time-series at specific locations due to the lack of spatially distributed reference data. Because of this restriction, the predictive power of these models, with regard to predicted spatial patterns, can usually not be judged.

An example of spatial predictions in hydrology is the prediction of saturated areas in agricultural catchments. These areas can be important source areas for the transport of agrochemicals to the stream. We set up a spatially distributed model to predict saturated areas in a 1.2 km^2 catchment in Switzerland with moderate topography. Around 40 % of the catchment area are artificially drained. We measured weather data, discharge and groundwater levels in 11 piezometers for 1.5 yr. For broadening the spatially distributed data sets that can be used for model calibration and validation, we translated soil morphological data available from soil maps into an estimate of the duration of soil saturation in the soil horizons. We used redox-morphology signs for these estimates. This resulted in a data set with high spatial coverage on which the model predictions were validated. In general, these saturation estimates corresponded well to the measured groundwater levels.

We worked with a model that would be applicable for management decisions because of its fast calculation speed and rather low data requirements. We simultaneously calibrated the model to the groundwater levels in the piezometers and discharge. The model was able to reproduce the general hydrological behavior of the catchment in terms of discharge and absolute groundwater levels. However, the accuracy of the groundwater level predictions was not high enough to be used for the prediction of saturated areas. The groundwater level dynamics were not adequately reproduced and the predicted spatial patterns of soil saturation did not correspond to the patterns estimated from the soil map. Our results indicate that an accurate prediction of the groundwater

HESSD

10, 12905–12950, 2013

level dynamics of the shallow groundwater in our catchment that is subject to artificial drainage would require a more complex model. Especially high spatial resolution and very detailed process representations at the boundary between the unsaturated and the saturated zone are expected to be crucial. The data needed for such a detailed model are not generally available. The high computational demand and the complex model setup would require more resources than the direct identification of saturated areas in the field. This severely hampers the practical use of such models despite their usefulness for scientific purposes.

1 Introduction

Spatially distributed hydrological models are popular tools in hydrology. They are claimed to be useful for supporting decisions in water resources management (e.g. Lyon et al., 2006; Heathwaite et al., 2005; Frey et al., 2009; Agnew et al., 2006). Despite the high spatial resolution of the computed variables, calibration and validation is often carried out only on discharge time-series at specific locations due to the lack of spatially distributed reference data (Srinivasan and McDowell, 2009). Furthermore, distributed models typically have a large computational demand because calculations are performed on several ten or hundred thousand cells. This huge resource requirement prevents meaningful uncertainty analysis that would require ten thousands of model runs. The predictive power of these models, with regard to predicted spatial patterns, can usually not be judged because of these restrictions.

An application of spatial predictions in hydrology is the prediction of critical source areas (CSAs) for diffuse pollution in agricultural areas. Herbicides are compounds for which diffuse pollution is important. Herbicides are widely used in agriculture and they can enter streams during rain events (e.g. Thurman et al., 1991; Wittmer et al., 2010; Leu et al., 2004a; Rabiet et al., 2010; Domagalski et al., 2008), where they can harm aquatic organisms even in low concentrations. Small streams in catchments with intensive crop production are especially at risk (Liess and Schulz, 1999), as dif-

HESSD
10, 12905–12950, 2013

fuse pollution from agricultural fields causes major inputs to the stream in these areas (Leu et al., 2010). Several studies have shown that the contributions of different fields within a catchment to the total herbicide load in the stream can differ significantly (Gomides Freitas et al., 2008; Leu et al., 2004b; Louchart et al., 2001). This implies that a relatively small proportion of a catchment can cause the major part of surface water pollution with herbicides. These areas are called critical source areas or contributing areas (Pionke et al., 1996). An area has to fulfill three conditions to become a critical source area: (1) the area needs to be a substance source; for herbicides all treated arable fields are source areas. (2) The area has to be hydrologically active. For herbicides, this means areas where surface runoff and/or macropore flow occur. (3) The area has to be connected to the stream; for herbicides this implies that the overland flow or macropore flow with the mobilized herbicides has to reach the stream without re-infiltration within the catchment (Pionke et al., 1996).

If CSAs can be reliably predicted, this offers efficient mitigation options, because actions on a small proportion of the area can strongly reduce the substance input to the stream. Basically there are two strategies to identify CSAs. They can be identified in the field or predicted with a model that captures the dominant features of the underlying mechanisms. The identification in the field is rather time consuming; it requires extensive field visits by experts and interviews with the local farmers. A model prediction can have advantages over the field identification with respect to the consistency of the CSA identification in a larger area and time demand.

Several studies have been carried out to predict CSAs for different substances (nutrients, pesticides and sediment) on field and catchment scale (e.g. Srinivasan and McDowell, 2009; Lyon et al., 2006; Heathwaite et al., 2005; Agnew et al., 2006) with a variety of different modeling approaches (see Borah and Bera, 2003, for review on model concepts for diffuse pollution). Process based models were found to be more suitable for CSA prediction by Srinivasan and McDowell (2009).

If the herbicide application patterns are known, the prediction of CSAs for herbicides reduces to a purely hydrological problem where the hydrologically active areas and

HESSD
10, 12905–12950, 2013

their connectivity to the stream have to be predicted. In this paper we focus on the prediction of areas that can become saturated and produce saturation excess overland flow because of high groundwater levels. Previous studies have demonstrated the relevance of this process for herbicide transport under conditions prevailing in the Swiss Plateau (Leu et al., 2004a). In contrast to areas where infiltration excess overland flow occurs, the locations of saturation excess overland flow areas on agricultural fields are temporally more stable across rainfall events of similar magnitude. This is because saturation excess areas on agricultural fields do not strongly depend on the land management and soil coverage. They are more influenced by their topographic position and hydrological subsoil properties (Lyon et al., 2006; Gerits et al., 1990; Doppler et al., 2012).

A main problem with the prediction of CSAs is the lack of spatial data on hydrological state variables. Predicting hydrological conditions that generate CSAs would require a physically-based, fully distributed modeling of catchment hydrology. Such models – like SHE (Abbott et al., 1986) and its derivatives – could theoretically be applied without calibration given full catchment information. However, since it is not possible to get full spatial information on catchment structure and status and because there are still considerable knowledge gaps (Refsgaard et al., 2010), spatially distributed models are often calibrated on aggregate data (like discharge measurements at specific locations). However, the model parameters and even the model structure are only poorly identifiable when no spatial data are used for calibration (Grayson et al., 1992a, b). For several versions of the semi-distributed TOPMODEL it was shown that especially the transmissivity parameter can be better identified if spatial data on groundwater levels or saturated areas were included for calibration (Franks et al., 1998; Lamb et al., 1998; Freer et al., 2004; Blazkova et al., 2002; Gallart et al., 2007).

Soil maps are a spatial data base that exists for many locations. Besides soil texture information, also the qualitative information on soil types contained in soil maps can be used in the context of hydrological models. Hrachowitz et al. (2013) state that hydrologically meaningful soil classification schemes are valuable for hydrological mod-

HESSD
10, 12905–12950, 2013

eling. Boorman et al. (1995) developed the system of Hydrology Of Soil Types (HOST) where soils in the UK are classified according to a conceptual understanding of the water movement in these soils. It was shown that the HOST soil classes are related to the base flow index (the proportion of base flow on total stream flow). This system was successfully implemented in a hydrological model (Maréchal and Holman, 2005). The HOST system has also proven to be useful for a hydrological soil classification at European scale (Schneider et al., 2007). In addition to the development of conceptual hydrological understanding, as it was done in HOST, soil morphology information was also used to critically evaluate spatial model predictions. For example Güntner et al. (2004) used soil morphological and geobotanical criteria to delineate saturated areas in a mesoscale catchment to evaluate the predictions by different terrain indices.

Despite these efforts to make use of available spatial information, the general lack of available spatial data sets to calibrate and/or validate models that predict CSAs still remains (Srinivasan and McDowell, 2009; Easton et al., 2008; Frey et al., 2011). For the prediction of CSAs this is critical since the prediction goal is the location where certain hydrological processes occur. Especially if management decisions should be based on predicted CSAs a meaningful model calibration and validation is warranted.

We present an approach where we used soil morphology information from a traditional soil map to derive estimates of the average duration of soil saturation at a given depth. The resulting data set can then be used as model validation data. The rationale behind this approach is the fact that groundwater influences morphological features that are related to changing oxygen availability due to permanent water logging or fluctuating groundwater levels. These hydromorphic features are usually related to redox reactions and transport of iron and manganese (see e.g. Terribile et al., 2011). Accordingly, soil morphology as described in soil maps contains information on the soil water regime. Several studies have shown a relationship between soil morphology (especially soil matrix color and the presence and type of iron mottles) and the frequency of soil saturation (Simonson and Boersma, 1972; Jacobs et al., 2002; Morgan and Stolt, 2006; Franzmeier et al., 1983). To our knowledge these morphological features

HESSD
10, 12905–12950, 2013

have only been interpreted as binary information (saturated area or not saturated area) (Güntner et al., 2004) but not as quantitative estimates (frequency of soil saturation). To do so, one has to be aware of possible pitfalls related to a quantitative interpretation of soil morphology. These features depend on various factors like the composition of the parent material (Evans and Franzmeier, 1986; Franzmeier et al., 1983), soil texture (Jacobs et al., 2002; Morgan and Stolt, 2006) and soil chemistry (Terribile et al., 2011; Vepraskas and Wilding, 1983). Also, artificial drainage can influence soil morphology within decades (Montagne et al., 2009; Hayes and Vepraskas, 2000). We have tried to account for these uncertainties by the extensive field experience for soil mapping in this part of Switzerland by some of us (PW, UZ). The resulting map of soil saturation durations itself could serve as proxy map for the identification of areas where saturation excess runoff occurs. However, in combination with a model it could be used for a more detailed prediction with respect to the time of the year in which the saturation occurs or the amount of runoff produced on a certain area. Even if the resulting map of soil saturation frequencies remains uncertain to some degree, this additional information can reduce the uncertainty of model predictions (Franks et al., 1998).

If a model prediction of CSAs should serve as basis for site specific pollution mitigation measures, it has to fulfill several criteria. It has to be reliable and its uncertainties have to be assessable. It should only be based on information that is generally available and it has to be applicable to larger areas. At the same time the scale of the prediction should be in the order of 10 m × 10 m (or smaller). The relevant transport processes for pesticides happen on the timescale of single events. A temporal resolution in the order of hours is therefore required for a dynamic prediction model. These requirements cause a high computational demand. Furthermore, the desired accuracy for the prediction of the groundwater level is high. It needs to distinguish between areas that are often saturated to the surface and therefore produce surface runoff, and areas where the maximum groundwater level remains little below the surface.

Hence, in this paper we describe a case study where we applied a spatially distributed hydrological model for delineating CSAs that are caused by the generation of

HESSD
10, 12905–12950, 2013

saturation excess overland flow due to high groundwater levels. Similar to Frey et al. (2009) we chose to work with a process oriented model, which has the advantage that it is better transferable to other regions than models that rely on empirical relationships. The model was optimized for computational speed and mainly relies on generally available data so that it could be used for practical applications. As study site we selected a 1.2 km^2 catchment in the Swiss Plateau, with a high variability of soil types and soil moisture regimes ranging from very wet to rather dry soils. One question we try to answer in this paper is if the spatial variability of depth to groundwater in this catchment can be explained only by topography and the presence of tile drains or if other factors like hydraulic soil properties are important driving factors in determining the groudwater levels. The frequency of soil saturation resulting from the quantitative interpretation of the soil map was not used for the model setup but only to critically evaluate the model predictions.

This case study therefore investigates whether dynamic, spatially distributed hydrological models can be used for the prediction of critical source areas so that land management decisions can be based on these predictions. Furthermore, we present an approach to increase the spatial information on soil water regimes. Soil morphological information was translated into spatially distributed data on water saturation as a function of soil depth in the study catchment. The result of this translation is a spatially distributed data set on the soil water regime which is based on generally available information. We used this data set to validate the spatial model predictions.

2 Materials and methods

2.1 Site description

The study catchment (1.2 km^2) is located in the northeast of Switzerland (see Fig. 1). Topography is moderate with altitudes ranging from 423 to 477 m a.s.l. and an average slope of 4.3° (min = 0°, max = 42°, based on 2 m × 2 m digital elevation model (DEM), ab-

HESSD
10, 12905–12950, 2013

solute accuracy: σ = 0.5 m, resolution = 1 cm, swisstopo, 2003). The twenty year mean annual precipitation at the closest permanent measurement station (Schaffhausen, 11 km north of the catchment) is 883 mm (Meteoschweiz, 2009). The soils have developed on moraine material with a thickness of around ten meters; underneath the moraine, we find fresh water molasse (Süsswassermolasse) (swisstopo, 2007; Einsele, 2000). Soils in the center of the catchment are poorly drained gleysols. In the higher parts of the catchment well drained cambisols and eroded regosols are found (FAL, 1997, see Fig. 1). Soil thickness (surface to C horizon) varies between 30 cm at the eroded locations and more than 2 m in the depressions and near the stream. The catchment is heavily modified by human activities; it encompasses a road network with a total length of 11.5 km (approximately 3 km are paved and drained, the rest is unpaved and not drained). The dominant land use is crop production (75 % of the area), around 13 % of the catchment is covered by forest, and a small settlement area is located in the southeast of the catchment. Three farms lie at least partly within the catchment (Fig. 1). 47 % of the agricultural land is drained by tile drains with a total length of over 21 km (Gemeinde Ossingen, 1995), the open stream has a length of 550 m. The main part of the drainage system was built in the 1930s. The stream system consists of two branches, an open ditch that was partly built as recipient for the drainage water, and the main branch of the stream that runs in a culvert (Fig. 1). The stream also receives the runoff from two main roads and from two farm yards (Gemeinde Ossingen, 2008). The paved area that drains into the catchment is approximately 1.5 ha (1.2 % of the area).

2.2 Field measurements

From 25 August 2008 to 14 October 2009, we monitored several hydrological variables in the catchment. We measured discharge at the outlet of the catchment (Fig. 1). Water level and flow velocity were measured using a Doppler probe and a pressure transducer (ISCO 750 area velocity flow module, Teledyne Inc., Los Angeles). Discharge was calculated using the exact cross section of the site. Discharge data were stored at

HESSD
10, 12905–12950, 2013

five-minute intervals by the data logger of an auto sampler (ISCO 6700, ISCO 6712, Teledyne Inc., Los Angeles USA).

At weather station A (Fig. 1), precipitation was measured at 15 min resolution with a tipping bucket rain gauge (R102, Campbell Scientific, Inc., Loughborough UK). This rain gauge was out of order for 22 days (4 June 2009–25 June 2009). During this time, rain data from weather station B (Fig. 1) were used (a mobile HP 100 Station run by Agroscope ART Reckenholz, CH with a tipping bucket rain gauge: HP 100, Lufft GmbH, Fellbach Germany). At weather station A we also recorded air temperature and relative humidity (Hygromer MP 100A, rotronic AG, Bassersdorf CH), wind speed (A100R switching anemometer, Campbell Scientific, Inc., Loughborough UK), net radiation (Q-7 net radiometer, Campbell Scientific, Inc., Loughborough UK) and air pressure (Keller DCX-22, KELLER AG für Druckmesstechnik, Winterthur CH) in 15 min intervals. Daily reference evapotranspiration was calculated from the meteorological data after the FAO Penman–Monteith equation (Allen et al., 1998). This results in the evapotranspiration of a reference grass surface without water limitation.

We installed 11 piezometers (Fig. 1) to monitor groundwater levels in 15 min intervals (STS DL/N, STS Sensor Technik Sirnach AG, Sirnach CH and Keller DCX-22, KELLER AG für Druckmesstechnik, Winterthur CH). The installation depth varied between 1.5 and 2.7 m below the surface. At four of the piezometer locations, we additionally dug a 1.2 m deep soil pit (Fig. 1) to directly investigate hydromorphic features.

2.3 GIS analysis

The catchment boundary was calculated in ArcGIS (ESRI, ArcGIS Desktop, 9.3.1) based on the 2 m × 2 m DEM (swisstopo, 2003) and manually adapted according to field observations, the detailed tile drain map (Gemeinde Ossingen, 1995) and the rain sewer map (Gemeinde Ossingen, 2008). The topographical catchment does not coincide completely with the subsurface catchment. In some areas that belong to the topographical catchment, the tile drains divert the water outside of the catchment. These areas were excluded. In contrast, the settlement area in the southeast was kept in

HESSD
10, 12905–12950, 2013

the catchment, even though the water from sealed areas in the settlement leaves the catchment.

The original 2 m × 2 m DEM (swisstopo, 2003) was used for the analysis of surface connectivity. Firstly, very small or shallow depressions were removed as these can either be artifacts in the DEM or are too shallow to trap significant amounts of overland flow. Depressions consisting of one or two cells and those with a maximum depth of less than 5 cm were filled. All other depressions were kept. Secondly, the cells in the open stream were incised to the depth of the average water level. Depression analysis and filling as well as stream incision were performed in TAS (TAS geographical information system version 2.0.9, John Lindsey 2005). Based on this corrected DEM, flow directions and flow accumulation were calculated in ArcGIS. The lowest stream channel cell was used as pour point for the catchment calculation to determine the area connected directly to the stream on the surface.

The corrected DEM was also used as surface topography in the model. The topographic wetness index was calculated with the D_{∞} algorithm implemented in TAS, based on the corrected DEM.

2.4 Soil map translation

We worked with the 1 : 5000 soil map of Canton Zurich (FAL, 1997). The soil map classifies agricultural soils after the Swiss soil classification system (FAL, 1997); forest soils are not classified. The soils are characterized according to their physical, chemical and morphological properties. For the estimation of the duration of soil saturation, the soil units (Fig. 1) were grouped into seven water regime classes, according to their expected water regime. For each of these classes we estimated how long it is saturated in six different depths (5, 30, 50, 75, 105, 135 cm). We used the following morphological redox features to estimate the duration of soil saturation within a soil horizon: (i) the presence and abundance of manganese concretions in the horizon, (ii) the presence and abundance of iron mottles, (iii) the presence of iron mottles together with pale soil matrix, and (iv) fully reduced horizons. These features of the horizons were interpreted

HESSD
10, 12905–12950, 2013

within the context of the respective soil profile and the expected water regime of the soil water regime class. Since variations are expected within the classes and because the estimation itself is uncertain, we additionally estimated a range of soil saturation in which we expect two thirds of the soils that are classified in the respective class.

2.5 Model description

2.5.1 Model concept

The model we worked with has a conceptual representation of the unsaturated zone and a spatially distributed, more process based representation of the saturated zone. Under wet temperate climate lateral flow in the saturated zone is an important process to determine the shape of the groundwater table in shallow groundwaters and therefore the prediction of saturated areas. For the saturated zone we chose an approach similar to HillVI (Weiler and McDonnell, 2004) where the groundwater level gradients are calculated in each time step and do not rely on surface topography. This should result in more realistic predictions of the location of saturated areas (Grabs et al., 2009). We additionally implemented the lateral and preferential flow to tile drains. These are important processes because large parts of the crop production areas in Switzerland are artificially drained.

The model simulates water fluxes in a catchment. It is based on the following water balance equation:

$$\frac{\mathrm{d}S}{\mathrm{d}t} = P - \mathrm{ET} - Q \tag{1}$$

with S [L] being the total water storage in the catchment, P [$\mathrm{L\,T^{-1}}$] is precipitation, ET [$\mathrm{L\,T^{-1}}$] is evapotranspiration and Q [$\mathrm{L\,T^{-1}}$] is stream discharge. We do not consider subsurface in- or outflow. The calculations were optimized for computational speed.

The model consists of three separate, linked modules (Fig. 2):

HESSD
10, 12905–12950, 2013

1. The paved area module is a lumped and conceptual model that calculates runoff and evaporation from paved areas.

2. The unsaturated zone module calculates recharge from the unsaturated zone to the saturated zone, preferential flow that bypasses the unsaturated zone and directly enters the saturated zone, and evapotranspiration from the unsaturated zone. It is possible to have several unsaturated zone modules (e.g. one for each soil type), each of which recharges into different sections of the saturated zone module.

3. The saturated zone module is spatially distributed (grid cells) and more process based. It simulates lateral groundwater flow, drain flow, evapotranspiration from the saturated zone, and saturation excess overland flow. The concept of the saturated zone module was inspired by HillVi (Weiler and McDonnell, 2004).

The modeled stream discharge consists of the following components:

$$Q = Q_{\text{paved}} + Q_{\text{surf}} + D_{\text{lat}} + D_{\text{pref}} \quad (2)$$

where Q_{paved} [$\text{L}\,\text{T}^{-1}$] is runoff from the paved area, Q_{surf} [$\text{L}\,\text{T}^{-1}$] is saturation excess surface runoff (this term also comprises lateral groundwater flow to the stream, see below), D_{lat} [$\text{L}\,\text{T}^{-1}$] is lateral drainflow, and D_{pref} [$\text{L}\,\text{T}^{-1}$] is preferential drainflow.

The modeled evapotranspiration is calculated as follows:

$$\text{ET} = E_{\text{paved}} + \text{ET}_{\text{uns}} + \text{ET}_{\text{sat}} \quad (3)$$

where E_{paved} [$\text{L}\,\text{T}^{-1}$] is the evaporation from paved areas, ET_{uns} [$\text{L}\,\text{T}^{-1}$] is the evapotranspiration from the unsaturated zone, and ET_{sat} [$\text{L}\,\text{T}^{-1}$] is the evapotranspiration from the saturated layer. In the following the three modules are described in detail.

HESSD
10, 12905–12950, 2013

Paved area module

The change in the paved storage is modeled as follows:

$$\frac{dS_{paved}}{dt} = P - E_{paved} - Q_{paved} \quad (4)$$

with S_{paved} [L] being the paved storage.

Runoff from paved areas linearly depends on the paved storage.

$$Q_{paved} = \begin{cases} 0 & \text{if } S_{paved} \leq S_{paved\_min} \\ (S_{paved} - S_{paved\_min})k_{paved} & \text{if } S_{paved} > S_{paved\_min} \end{cases} \quad (5)$$

S_{paved_min} [L] is the minimum storage that has to be filled to produce runoff and k_{paved} [T^{-1}] is the outflow rate.

If there is water in the paved storage, it can evaporate with the following rate

$$E_{paved} = ET_{ref} \cdot m_{paved} \quad (6)$$

where ET_{ref} [LT^{-1}] is the reference evapotranspiration calculated from meteorological data (see Sect.2.2), and m_{paved} [-] is a multiplier.

Unsaturated zone module

The water balance of the unsaturated zone is represented as follows:

$$\frac{dS_{uns}}{dt} = P - ET_{uns} - R \quad (7)$$

where S_{uns} [L] is the unsaturated storage, and R [LT^{-1}] is recharge to the saturated zone. R consists of a slow recharge component (R_{slow}) and preferential flow (R_{pref}).

$$R = R_{slow} + R_{pref} \quad (8)$$

HESSD
10, 12905–12950, 2013

R_{slow} linearly depends on the storage amount above field capacity. If the unsaturated storage is below field capacity, R_{slow} is assumed to be zero.

$$R_{slow} = \begin{cases} 0 & \text{if } S_{uns} < S_{fc} \\ (S_{uns} - S_{fc})k_{uns} & \text{if } S_{uns} \geq S_{fc} \end{cases} \quad (9)$$

S_{fc} [L] is the unsaturated store at field capacity and k_{uns} [T^{-1}] is the outflow rate.

A part of the precipitation bypasses the unsaturated zone as preferential flow and directly enters the saturated zone. This only occurs if the unsaturated zone is above field capacity, and it exponentially depends on the water content in the unsaturated zone.

$$R_{pref} = \begin{cases} 0 & \text{if } S_{uns} < S_{fc} \\ k_{pref}\left(\frac{S_{uns}-S_{fc}}{S_{uns\_max}-S_{fc}}\right)^{e_{pref}} \cdot P & \text{if } S_{uns} \geq S_{fc} \end{cases} \quad (10)$$

k_{pref} [-] and e_{pref} [-] are empirical parameters.

Above field capacity the evapotranspiration from the unsaturated module is at maximum, below field capacity it is reduced. The reference evapotranspiration calculated from meteorological data (ET_{ref}) refers to a reference grass surface. A time dependent multiplier (m_{uns}) was introduced to account for crops with different water requirements and the time dependence of the leaf area index (LAI) due to crop development.

$$ET_{uns} = \begin{cases} ET_{ref} \cdot m_{uns} & \text{if } S_{uns} \geq S_{fc} \\ ET_{ref} \cdot m_{uns} \left(\frac{\frac{S_{uns}}{S_{fc}}}{\frac{S_{uns}}{S_{fc}} + k_{et}}\right)(1 + k_{et}) & \text{if } S_{uns} < S_{fc} \end{cases} \quad (11)$$

HESSD
10, 12905–12950, 2013

with k_{et} [-] and m_{uns} [-] being parameters. The change of the LAI is coupled to air temperature and incorporated in the time dependent parameter m_{uns}.

$$\frac{dm_{uns}}{dt} = \begin{cases} m_{uns} \cdot \mu_0 (T_{air} - T_0) \left(1 - \frac{m_{uns}}{m_{uns,\,max}}\right) & \text{if } T_{air} \geq T_0 \\ m_{uns} \cdot k_{decay} (T_{air} - T_0) & \text{if } T_{air} < T_0 \\ 0 & \text{if } m_{uns} \leq m_{uns,\,min} \end{cases} \quad (12)$$

where μ_0 [T^{-1} Te^{-1}] and k_{decay} [T^{-1} Te^{-1}] are parameters, T_{air} [Te] is air temperature, T_0 [Te] is the minimum temperature above which LAI starts increasing, $m_{uns,\,min}$ [-] and $m_{uns,\,max}$ [-] are the minimum and maximum values for m_{uns}.

Saturated zone module

The saturated module is spatially distributed. The water balance within a grid-cell is calculated as follows:

$$\frac{dS_{sat}}{dt} = R - ET_{sat} + SF_{lat} - i \cdot D_{lat} - i \cdot D_{pref} - j \cdot Q_{surf} \quad (13)$$

where S_{sat} [L] is the storage in the cell and SF_{lat} [LT^{-1}] is the lateral groundwater flow between cells.

$$i = \begin{cases} 1 & \text{for drained cells} \\ 0 & \text{for undrained cells} \end{cases} \quad (14)$$

$$j = \begin{cases} 1 & \text{for cells with surface connectivity to the stream, see Sect. 2.3} \\ 0 & \text{for cells without surface connectivity to the stream} \end{cases} \quad (15)$$

The change of the groundwater level in the cell is therefore calculated as follows

$$\frac{dh}{dt} = \frac{\frac{dS_{sat}}{dt}}{p_{eff}} \quad (16)$$

HESSD
10, 12905–12950, 2013

where h [L] is the groundwater level and p_{eff} [-] is the effective porosity.

If the unsaturated zone is below field capacity and evapotranspiration from the unsaturated zone is therefore reduced, evapotranspiration can occur directly from the saturated zone.

$$\text{ET}_{\text{sat}} = \begin{cases} 0 & \text{if } S_{\text{uns}} \geq S_{\text{fc}} \\ m_{\text{sat}}(\text{ET}_{\text{ref}} \cdot m_{\text{uns}} - \text{ET}_{\text{uns}}) & \text{if } S_{\text{uns}} < S_{\text{fc}} \end{cases} \quad (17)$$

At maximum, ET_{sat} accounts for the evapotranspiration deficit in the unsaturated zone, the multiplier m_{sat} [-] is between 0 and 1.

The lateral groundwater flow between cells is calculated based on the Dupuit–Forchheimer assumption. We furthermore assume isotropy in K_{sat}:

$$q_{\text{lat}} = K_{\text{sat}} \cdot \nabla h \quad (18)$$

where q_{lat} [$\text{L}\,\text{T}^{-1}$] is the flux density, K_{sat} [$\text{L}\,\text{T}^{-1}$] is the saturated hydraulic conductivity, and h [L] is the groundwater head. The water flow between two neighboring cells can then be calculated as follows:

$$Q_{\text{lat}} = K_{\text{sat}} \cdot M_{\text{sat}} \cdot L_{\text{cell}} \frac{\Delta h}{L_{\text{cell}}} \quad (19)$$

where Q_{lat} [$\text{L}^3\,\text{T}^{-1}$] is the water flow between two cells, M_{sat} [L] is the thickness of the saturated layer, and L_{cell} [L] is the cell length. If we sum up the water flows to and from all neighboring cells and divide the sum by the cell area, we receive SF_{lat}.

In drained cells, the lateral groundwater flow into the drain is calculated based on the Hooghoudt equation as described by Beers (1976). We used an equation modified from Wittmer (2010) because the distance to single tiles is not considered explicitly. The flow depends on the water level above the drains.

$$D_{\text{lat}} = 4 r_{\text{dr}} \cdot K_{\text{sat}} \left(\frac{m_{\text{dr}} \cdot H_{\text{dr}}}{\text{Sp}_{\text{dr}}} \right)^2 \quad (20)$$

HESSD
10, 12905–12950, 2013

D_{lat} [L T^{-1}] is the drainflow, r_{dr} [-] is a parameter that determines the entrance resistance to the tile drains, m_{dr} [-] is a multiplier to obtain the water level in the middle between two drains from the modeled water level in the cell, H_{dr} [L] is the water table height above the drain, and Sp_{dr} [L] is the drain spacing.

If the groundwater level reaches the surface in a cell, three cases are distinguished:

1. The cell is directly connected to the stream on the surface (see Sect. 2.3). In this case all water above the surface is directly added to discharge (Q_{surf}).

2. The cell is not connected but it is drained. In this case, all water above the surface is added to drainflow as preferential flow (D_{pref}).

3. The cell is neither connected to the stream nor drained. The water remains in the cell.

The coupling between the saturated zone module and the unsaturated zone module is unidirectional from the unsaturated zone to the saturated zone. The fact that a cell is saturated to the surface does therefore not influence the unsaturated zone module above it. It is possible that the unsaturated zone above a saturated cell is not completely full. This concept was chosen to achieve a high computational efficiency.

The stream channel cells are incised to a mean water level in the stream. The surface topography in the stream cells is therefore represented by the mean water level and all the water above this level in the cell is directly converted to discharge. Lateral groundwater flow to stream cells is therefore also converted to Q_{surf}.

2.5.2 Model setup

We ran the model with homogeneous hydraulic properties in the saturated zone, only topography and the presence of tile drains where spatially distributed. The unsaturated zone was divided into several classes according to land use (forest, settlement, agriculture) and, within agricultural landuse, according to the seven soil categories (see

HESSD
10, 12905–12950, 2013

Sect. 2.4). We therefore ended up with nine unsaturated zone classes (forest, settlement and the seven soil categories). The reason for this setup was the assumption that the groundwater level in the catchment is mainly influenced by topography and artificial drainage and not by hydraulic soil properties (soil texture is rather homogeneous within the catchment (FAL, 1997)). However, to account for the spatial distribution of the unsaturated zone thickness (which also influences the other parameters of the unsaturated zone module), we divided the unsaturated zone into classes according to their soil water regime. The classification of soil water regimes was only used for the spatial division of the unsaturated zone (but not its parameterization).

The saturated zone was represented by a 16 m × 16 m grid; the cells were 10 m thick. We assume that the soil and the moraine are the conducting layers while the Fresh water molasse is assumed to be impermeable (see Sect. 2.1). The calculations were run with hourly input time series; the model output was also in hourly steps.

2.5.3 Implementation

The model equations were implemented in a C++ program to achieve fast model simulations. The ordinary differential equations of the conceptual unsaturated zone modules and the paved area module were numerically integrated with the LSODA solver package (Hindmarsh, 1983; Petzold, 1983). The partial differential equations of the saturated zone module were integrated with an explicit Euler solution scheme with a computational time-step (20 min) that guaranteed numerical stability during the simulation period. The integration of the saturated zone module was sped up by parallelizing the explicit solution scheme with OpenMP threads (for the specification see http://openmp.org). Despite all these efforts the simulation of the 2-D groundwater surface remained rather time consuming requiring 28 s of computation time for 1 yr of forward simulation on an Intel Core i7–3960X CPU (3.3 GHz).

Model implementation and model setup (e.g. spatial and temporal resolution) were chosen in a way that guaranteed simulations fast enough to allow a possible use for practical applications.

HESSD
10, 12905–12950, 2013

2.5.4 Calibration

The model was simultaneously calibrated to the discharge time series and the groundwater level time series in the eleven piezometers. A maximum likelihood approach was used. Discharge was Box–Cox transformed before calibration with $\lambda = 1/3$ (Box and Cox, 1964, 1982). The transformation equation was as follows:

$$g(x) = \frac{x^{\lambda} - 1}{\lambda} \tag{21}$$

We assumed independent and normally distributed errors for the transformed discharge and the groundwater levels; the standard deviations for these were also calibrated. The likelihood function therefore looked as follows:

$$L(\boldsymbol{\theta}, \boldsymbol{\sigma}) \propto \prod_{i=1}^{11} \prod_{j=1}^{m} \frac{1}{\sigma_i \sqrt{2\pi}} \exp\left(-\frac{1}{2} \left(\frac{O_i^j - M_i^j(\boldsymbol{\theta})}{\sigma_i} \right)^2 \right) \tag{22}$$
$$\times \prod_{j=1}^{m} \frac{1}{\sigma_d \sqrt{2\pi}} \exp\left(-\frac{1}{2} \left(\frac{g(O_d^j) - g(M_d^j(\boldsymbol{\theta}))}{\sigma_d} \right)^2 \right)$$

where L is the likelihood, $\boldsymbol{\theta}$ is the vector of model parameters, $\boldsymbol{\sigma}$ is the vector of the standard deviations, i are the 11 piezometer locations, j are the time-points, σ_i is the standard deviation at piezometer i, O_i^j is the observed groundwater level at piezometer i and time j, $M_i^j(\boldsymbol{\theta})$ is the modeled groundwater level at piezometer i and time j, σ_d is the standard deviation of the transformed discharge, $g(x)$ is the Box–Cox transformation (see above), O_d^j is the observed discharge at time j and $M_d^j(\boldsymbol{\theta})$ is the modeled discharge at time j.

During calibration the likelihood function was optimized with a coupled global-local algorithm. Optimization started with the Particle Swarm algorithm (Kennedy and Eber-

HESSD
10, 12905–12950, 2013

hart, 1995) and after reaching the stop criterion Nelder–Mead Simplex optimization (Nelder and Mead, 1965) was launched from the best parameter combination.

We chose a period in spring and summer 2009 as calibration period. It starts very wet in the beginning of spring, includes a long dry period, several rain events with varying magnitudes and intensities and it also contains the largest discharge event in the measurement period. We do not have continuous measurement time series from all the piezometers. For each piezometer we chose the calibration period so, that all the calibration time series (discharge and the 11 piezometers) contained the same number of observations. Most of the model parameters were calibrated to achieve the best possible model output with the given model structure. (The tables in the supporting information indicate which of the parameters were calibrated and which were kept fixed during calibration. The tables also indicate the minimum and maximum values that were allowed in the calibration.) The initial state of the unsaturated zone was calibrated as well. The initial condition for the groundwater level is difficult to calibrate because the shape of the surface depends on the model parameters. The model run was started five months before the calibration period to adapt the groundwater surface to the model parameters. Additionally, we added a parameter that allows a homogeneous shifting up or down of the groundwater initial state and chose an adaptive procedure. After a first calibration, we used a groundwater level map from the optimum parameter set as initial condition for a second calibration. In a first step we calibrated a model version with a homogeneous unsaturated zone. From the resulting optimum parameter set, we launched the calibration of the model version with the spatially distributed unsaturated zone. With this setup, one full optimization (global and local) took about one week depending on the speed of convergence.

HESSD
10, 12905–12950, 2013

3 Results

3.1 Saturation estimates

Figure 3a shows the map of the seven water regime classes from the reclassification of of the soil map. Class 1 is the driest, class 7 the wettest water regime class. In Fig. 4 the estimated saturation durations in the water regime classes are shown. To evaluate the map based estimates of the water regime we can compare the estimates with the measured groundwater levels from the piezometers (Fig. 4). In general, the estimated durations of soil saturation are in good agreement with the piezometers. There are some deviations at specific locations like the very wet piezometer in the driest soil class (piezometer 1 in Fig. 1 indicated by an arrow in Fig. 4). For a further evaluation of the spatial distribution of the water regime classes, we compared the water regime class map (Fig. 3a) with the topographic wetness index (Fig. 3b). The comparison reveals a generally good match between the two maps (high topoindex means wet soil). Even small scale features in the topoindex map are reflected in the soil map (e.g. in the NE of the catchment). For a quantitative comparison of the two maps, we classified the wettest two water regime classes (classes 6 and 7) as potential CSAs. This resulted in 20 % of the area classified as CSA. For the topoindex map we also classified the wettest 20 % as CSA. The areal overlap of the CSAs from the two methods is 52 %. Despite this reasonable agreement between the two maps there are some areas with rather high topoindices where the soils are classified in dry soil classes (e.g. in the west of the catchment).

The location of tile drains also contains information on the soil water regime. The tile drain map can therefore be used as additional comparison to plausibilize the soil map estimates. Tile drains are only present at locations with excess groundwater that has to be diverted. Drained areas are therefore good indicators of originally higher groundwater levels. Because the drains are installed between 1 and 1.5 m below the surface in the study catchment, groundwater levels are still expected to be rather high in drained areas. We therefore used the drainage map (Fig. 3c) as a further evaluation

HESSD
10, 12905–12950, 2013

of the map of soil water regime classes. The comparison reveals that drained areas are areas with high topographic indices and that the drained soils are usually classified into a wet water regime class. However, the western part of the catchment is intensely drained and has rather high topographic wetness indices, but large areas are classified in the driest water regime class. Also the wet piezometer in water regime class 1 (Fig. 4, indicated by an arrow) is located in this area. The local assessment in the soil pit besides piezometer 1 (Fig. 1) supports the map based estimate. Only few small iron mottles were found below 1 m. The piezometric measurement therefore contradicts the local morphological interpretation in the soil pit and the map based estimate. This is the only soil pit location where this is the case, in the other three soil pits (Fig. 1) the piezometric measurement, the local morphological interpretation in the soil pit and the map based estimate corresponded well.

3.2 Calibration results and model validation

After calibration (the optimum parameter set can be found in the supporting information), the model performed satisfactory with respect to discharge and absolute groundwater levels. Figure 5 shows the predicted and measured discharge time-series. The bad fit in the beginning stems from the difficulty to calibrate the initial groundwater level (see Sect. 2.5.4). After this initial phase, the discharge prediction is good with a Nash–Sutcliffe coefficient (Nash and Sutcliffe, 1970) of 0.91 for the calibration period. Also the predicted average groundwater levels at the piezometer locations are in good agreement with the measurements (Fig. 6). After the initial phase, the difference between modeled and measured groundwater level is usually less than one meter. The model was therefore able to reproduce the general hydrological behavior of the catchment. Also the modeled composition of the discharge, with most of the discharge originating from the drainage system, was in good agreement with the measurements (data not shown).

However, if the timeseries of the groundwater levels are plotted as depth below the soil surface (Fig. 7) it becomes obvious that there is a lack of groundwater level dynam-

HESSD
10, 12905–12950, 2013

ics in the model. The observed groundwater levels are much more dynamic than the modeled ones. Additionally, Fig. 7 shows that the depth to groundwater in the model prediction is rather homogeneous throughout the area. The modeled average depth to groundwater does not vary much between the piezometer locations. In contrast, the measured depth to groundwater is more variable.

To further investigate the model performance with respect to the spatial distribution of groundwater levels we used the estimated saturation durations from the soil map (Fig. 8). This allowed a model evaluation at locations without measurements and at locations where the model was not calibrated to. Figure 8 shows that the model does not differentiate between the water regime classes. In all the classes, there are dry and wet model cells. As a general behavior, the model represents the dry locations (water regime class 1) too wet and the wet locations (water regime classes 6 and 7) too dry. However, the model was able to predict the areas with the lowest groundwater levels. Model cells where the modeled groundwater level is deeper than three meters below the surface are only located in water regime class one (Fig. 8). Hence, the model was not able to reproduce the spatial variability in saturation durations, except for the locations with the lowest groundwater levels, even though it was calibrated on measured groundwater levels distributed throughout the catchment.

For a more complete picture of the modeled spatial distribution of the depth to groundwater in the catchment Fig. 9 shows a map of the model output from 27 July 2009. This is a situation with high groundwater levels after the largest rain event in the modeled period. Figure 9 reveals a clear dominance of the drainage system in the determination of the modeled groundwater level (compare Fig. 9 with Fig. 3c). This is also visible in Fig. 8. Most of the drained cells show a very similar behavior with stable groundwater levels around 1.5 m below the surface (the installation depth of the tile drains). A comparison of Fig. 9 with Fig. 3a shows that the spatial pattern of the model output does not resemble the pattern observed in soil morphology. The spatial overlap between the CSAs from the soil map (water regime classes 6 and 7) and the wettest 20 % of the cells in the modeled output is only 12 %. Model and soil map would

HESSD
10, 12905–12950, 2013

therefore predict completely different locations as CSAs. The model predicts high water tables in areas where it should be dry. In the center of the catchment, where the area is drained but still wet in reality, the model predicts too low water levels (compare Fig. 9 with Fig. 3c). It seems that the drainage system in the model is too efficient.

4 Discussion

4.1 Soil map translation

A meaningful validation of the saturation duration estimates from the soil map is not straight forward due to several difficulties. First, there are spatial aspects. The spatial coverage of the estimates corresponds to the soil map unit while piezometers are point measurements. Hence, deviations between soil map estimates and piezometer data may simply reflect local inhomogeneities. Furthermore, the soil map divides the area into units with sharp boundaries. Some of these boundaries are in reality gradual changes. The vicinity of a piezometer to a soil unit boundary can therefore hinder a meaningful evaluation. A second difficulty is that the estimates do not differ heavily; the saturation estimates change gradually from one class to the next. The piezometer measurements could therefore fit well in more than one class. Third, there are temporal aspects of the validation. Soil morphology does not necessarily reflect the current water regime, especially when the water regime has recently changed because of artificial drainage. According to Hayes and Vepraskas (2000), soil drainage can alter morphology within decades. Finally, it is possible that the morphological signs of wetness do not evolve in a certain soil, even though the same water regime persists since a longer time. A possibility for this is soil saturation without oxygen depletion (e.g. frequent but short periods of saturation), which does not lead to morphological changes (Evans and Franzmeier, 1986; Pickering and Veneman, 1984).

The main part of the drainage system in our study catchment was installed in the 1930ies, the soil map was produced between 1988 and 1997. It can therefore be ex-

HESSD
10, 12905–12950, 2013

pected that soil morphology reflects the current situation. However, the interpretation of drained soils will, in general, remain difficult.

The mismatch between the measured groundwater level and soil morphology at piezometer 1 shows the limitations of the approach. Soil morphology does not reflect the current water regime everywhere. The reasons for this can be manifold. As stated above, it is possible that the morphological signs of wetness did not evolve in this soil, even though the same water regime persists since a longer time. On the other hand, the current water regime as measured in the piezometer could have developed only few years ago, e.g. because of a poorly maintained and clogged part of the drainage system.

Despite these difficulties and limitations, the comparison of the estimates with the piezometric measurements shows a generally good agreement (Fig. 4). We are therefore confident that soil morphology in this region reflects the current water regime in most soils. The good agreement between the topographic wetness index and the map of the soil water regime classes indicates that the soil distribution with respect to soil saturation and soil water regime is mainly driven by topography in this catchment. In addition this correspondence shows that the estimation of soil saturation from soil map information resulted in a reasonable spatial pattern of soil saturation in this catchment.

The quantitative interpretation of soil morphology will always remain uncertain to some degree. However, if the uncertainties can be quantified, such information can still be very valuable for model calibration and evaluation (Franks et al., 1998).

4.2 Model predictions

We chose a model setup with a homogeneous saturated zone where every cell in the saturated zone module had the same parameters. The only spatially variable attributes in the saturated zone module were topography, surface connectivity and tile drainage. However, with the spatially distributed unsaturated zone our setup resulted in 83 parameters to calibrate. The optimization was therefore a rather complex problem with the simultaneous calibration to discharge and groundwater levels at eleven locations.

HESSD
10, 12905–12950, 2013

We started the calibration at the optimum parameter set of a model setup with a homogeneous unsaturated zone. Some of the parameters did not differentiate into the nine unsaturated zones but remained at the starting parameter value for all or some of the unsaturated zone modules. The likelihood function was therefore insensitive to a spatial distribution of these parameters (see supporting information for the table of the maximum likelihood parameter set).

The model is able to reproduce the general hydrological behavior of the catchment (Figs. 5 and 6). The good match between observed and modeled groundwater levels (Fig. 6) with a model that assumes homogeneous soil properties indicates that groundwater levels in this catchment are mainly driven by topography and are not strongly influenced by the variability of hydraulic soil properties. However, if we focus on the top two meters below soil surface there are some deficiencies in the groundwater level predictions. This implies that other factors than just topography influence the depth to groundwater at this detailed scale.

The comparison with the estimates of soil saturation reveals a lack of differentiation between wet and dry areas (Fig. 7) and wrong spatial patterns of soil saturation (Fig. 9). The main problems are (i) the missing dynamics in the groundwater levels, (ii) the dominance of the drainage system with respect to groundwater levels which leads to wrong spatial patterns of soil saturation and (iii) the homogeneity within the drained part of the catchment. These deficiencies are problematic if one wants to use such a model to predict critical source areas. Saturation excess overland flow only occurs in situations with high groundwater levels. A prediction model therefore needs to be able to adequately reproduce groundwater dynamics especially in situations with high groundwater levels. Furthermore, large parts of the intensively cultivated cropping areas in Switzerland are artificially drained; the model should therefore be able to predict groundwater levels and their dynamics in drained areas. The prediction of saturation excess areas requires a very high accuracy in groundwater level prediction. A difference of 50 cm or less in the depth to groundwater is already crucial, because it decides weather an area often produces saturation excess overland flow. When the absolute groundwater level range

HESSD
10, 12905–12950, 2013

within the catchment is more than 30 m, the prediction of 50 cm difference is a difficult task. Even though the model captured the general hydrological behavior of the catchment with respect to discharge and absolute groundwater levels, it was far from being useful as a prediction tool for saturated areas. It did not achieve the accuracy that is needed for practical applications.

Some of the deficiencies were possibly caused by the chosen model setup of decoupled unsaturated and saturated zone modules. The groundwater level dynamics could probably be improved with a fully coupled saturated – unsaturated model where the effective porosity could vary with depth and with the status of the unsaturated zone. In addition, the unsaturated zone module does not react to changes in the groundwater level, even though in reality the unsaturated zone storage shrinks with a rising groundwater level. (Water that was counted to the unsaturated zone storage before belongs to the saturated storage when the water level rises. The unsaturated zone becomes thinner and therefore contains less water.) (Seibert et al., 2003.) A further problem is the areal representation of the drainage system which is, in reality, a linear feature. The areal representation in the model prevents the buildup of high groundwater levels between drainage tubes and the corresponding high gradients between drainage tube and the undrained space between drainage tubes. If the tile drains should be implemented as linear features in a model, this would require a much higher spatial resolution. The rather low spatial resolution of our model setup (16 m) generally prevents the reproduction of very steep gradients on short distances which also influences the groundwater level dynamics.

These possible improvements of the model structure would lead to a three dimensional fully coupled saturated – unsaturated model with a high spatial resolution and a linear representation of the drainage system. It seems that such a detailed model would be necessary to achieve the accuracy which is necessary for the prediction of CSAs. A closer look at the piezometer data in Fig. 7 reveals that the groundwater level fluctuations are rather complex. Every piezometer reacts individually to the different rain events. Moreover, the dynamics of piezometers within the same water regime

HESSD
10, 12905–12950, 2013

class differ substantially. Even if we consider whether a piezometer location is drained or not, it is impossible to explain the differences and similarities of the groundwater dynamics. It would have been possible that the model can explain the spatial variability of groundwater level dynamics if these dynamics are determined by a combination of topographic position, the soil water regime class and the drained areas. However, the discrepancy between modeled and measured groundwater levels indicates that other processes influence the groundwater levels to a degree that can not be neglected. Even in the rather simple and homogeneous study catchment the fluctuations of the shallow groundwater seem to be complex. From a scientific point of view it would be interesting to dig deeper into these processes, trying to understand the influencing factors of the groundwater level dynamics with the help of a more complex model and a better spatial resolution. However, such a model would require very detailed information on the drainage system and its maintenance status. Besides, the computational demand for such a model would be very high when it is applied to the area of a whole catchment.

In the light of the above discussion about a more complex model it seems surprising that the prediction of CSAs by the topographic wetness index is in better agreement with the soil map than the predictions of the much more complex and realistic model. The assumptions behind the topographic wetness index are a groundwater level surface that is parallel to surface topography and the topo index totally ignores the tile drains. The added process understanding in our model where we included the tile drains, the unsaturated zone and a more realistic groundwater level surface calculation did not result in better spatial predictions. In contrast, the spatial predictions became worse. However, the topographic wetness index does not allow a quantitative analysis. Still, the rather good performance of the topographic wetness index with respect to spatial predictions indicates that a model of similar complexity and computational demand as ours might possibly be able to better predict CSAs and still have the advantages of a quantitative model prediction. Possibly we added model complexity at the wrong processes.

HESSD
10, 12905–12950, 2013

So far we discussed identification of CSAs caused by saturation excess overland flow. However, it was shown that areas that produce infiltration excess overland flow can be CSA on arable land (Doppler et al., 2012). These areas depend strongly on the actual land management and they can change with crop rotation or when the management practices are changing. Therefore, their identification requires knowledge on the current local site conditions. As an example, Srinivasan and McDowell (2009) found that small trampled areas beside fences were relevant in the occurrence of infiltration excess overland flow and the transport of phosphorus to the stream. Such features can not be captured by models based on generally available information and once they are identified in the field there is no need to implement them into a prediction model.

The focus of this study was to use a model that would be applicable for practical purposes. Besides model based predictions, critical source areas can also be directly identified in the field by experts. This requires interviews with the local farmers and detailed site inspections. If a prediction model for CSAs should serve as basis for pollution mitigation measures, it must have advantages as compared to field visits by experts. An advantage of model predictions would be that predictions can be based on existing knowledge, so that field visits would not be necessary. However, the need for very detailed knowledge (e.g. on the drainage system and on the actual land management) undoes this advantage. Additionally, the demanding setup of a very detailed model, its calibration and test in every small catchment (not to talk about uncertainty analysis) would not lead to a time gain compared to field visits by experts to directly identify CSAs in the field.

5 Conclusions and outlook

Our case study has shown that the estimation of saturation durations from morphological soil map information is possible and these estimates have proven to be useful for model validation even though the resulting map of duration of soil saturation remains uncertain to some degree because the estimates do not always represent the cur-

HESSD
10, 12905–12950, 2013

rent water regime. The additional data source provides quantitative spatial information on the soil water regime that can be used as validation data for the predicted spatial patterns. In a further step such estimates could also be used to calibrate spatially distributed hydrological models, so that no groundwater level measurements are needed for model calibration.

The model was able to reproduce the general hydrological behavior of the catchment. However, the desired accuracy of the groundwater level predictions – which is needed for the identification of CSAs – could not be achieved. The processes that determine the groundwater level dynamics in this catchment seem to be more complex than the used model. It seems that a high spatial resolution and very detailed process representations are needed for a groundwater level prediction that is accurate enough for the identification of CSAs in practical situations. Drained areas are especially challenging for the following reasons: limited data availability on tile drain locations and maintenance status; difficult integration in catchment models (concept and spatial resolution) and finally the estimation of soil saturation duration is much more difficult in drained areas.

Our results indicate that dynamic, spatially distributed hydrological models to predict CSAs are still far from being useful for management decisions. If a model should be accurate enough and should also include infiltration excess areas, it would require information that is not generally available. Furthermore, the setup and test of such a complex model would need more resources than direct observations of CSAs in the field by experts and the local farmers. If site specific management of CSAs should be achieved, we recommend to identify these areas in the field and not solely by model predictions. However, predictions by simple models like the topographic wetness index can be helpful for the identification of CSAs in the field. It would also be interesting to test the predictive capabilities of different modeling concepts under real world conditions.

HESSD
10, 12905–12950, 2013

Supplementary material related to this article is available online at http://www.hydrol-earth-syst-sci-discuss.net/10/12905/2013/hessd-10-12905-2013-supplement.pdf.

Acknowledgements. The field work would not have been possible without Ivo Strahm, Luca Winiger, Marcel Gay and Hans Wunderli. We also would like to acknowledge the local farmers for their cooperation. We gratefully acknowledge the funding by the Swiss Federal Office for the Environment (FOEN).

References

Abbott, M. B., Bathurst, J. C., Cunge, J. A., O'Connell, P. E., and Rasmussen, J.: An introduction to the European Hydrological System – Systeme Hydrologique Européen, "SHE", 1: history and philosophy of a physically-based, distributed modelling system, J. Hydrol., 87, 45–59, 1986. 12909

Agnew, L. J., Lyon, S., Gérard-Marchant, P., Collins, V. B., Lembo, A. J., Steenhuis, T. S., and Walter, M. T.: Identifying hydrologically sensitive areas: bridging the gap between science and application, J. Environ. Manage., 78, 63–76, 2006. 12907, 12908

Allen, R. G., Pereira, L. S., Raes, D., and Smith, M.: Crop evapotranspiration – Guidelines for computing crop water requirements – FAO Irrigation and drainage paper 56, FAO – Food and Agriculture Organization of the United Nations, Rome, 1998. 12914

Beers, W. F. J.: Computing drain spacings, Wageningen, International institute for land reclamation and improvement, 1976. 12921

Blazkova, S., Beven, K. J., and Kulasova, A.: On constraining TOPMODEL hydrograph simulations using partial saturated area information, Hydrol. Process., 16, 441–458, 2002. 12909

Boorman, D. B., Hollis, J. M., and Lilly, A.: Hydrology of soil types: a hydrologically-based classification of the soils of the United Kingdom, Inst. Hydrol., Wallingford, available at: http://www.ceh.ac.uk/products/publications/documents/ih126hydrologyofsoiltypes.pdf (last access: 28 October 2013), 1995. 12910

Borah, D. K. and Bera, M.: Watershed-scale hydrologic and nonpoint-source pollution models: review of mathematical bases, T. Asae, 46, 1553–1566, 2003. 12908

Box, G. E. P. and Cox, D. R.: An analysis of transformations, J. Roy. Stat. Soc. B, 26, 211–252, 1964. 12924
Box, G. E. P. and Cox, D. R.: An analysis of transformations revisited, rebutted, J. Am. Stat. Assoc., 77, 209–210, 1982. 12924
Domagalski, J. L., Ator, S., Coupe, R., McCarthy, K., Lampe, D., Sandstrom, M., and Baker, N.: Comparative study of transport processes of nitrogen, phosphorus, and herbicides to streams in five agricultural basins, USA, J. Environ. Qual., 37, 1158–1169, 2008. 12907
Doppler, T., Camenzuli, L., Hirzel, G., Krauss, M., Lück, A., and Stamm, C.: Spatial variability of herbicide mobilisation and transport at catchment scale: insights from a field experiment, Hydrol. Earth Syst. Sci., 16, 1947–1967, doi:10.5194/hess-16-1947-2012, 2012. 12909, 12934
Easton, Z. M., Fuka, D. R., Walter, M. T., Cowan, D. M., Schneiderman, E. M., and Steenhuis, T. S.: Re-conceptualizing the soil and water assessment tool (SWAT) model to predict runoff from variable source areas, J. Hydrol., 348, 279–291, 2008. 12910
Einsele, G: Sedimentary Basins: Evolution, Facies, and Sediment Budget, 2 Edn., Springer, Berlin, 2000. 12913
Evans, C. V. and Franzmeier, D. P.: Saturation, aeration, and color patterns in a toposequence of soils in North-Central Indiana, Soil Sci. Soc. Am. J., 50, 975–980, 1986. 12911, 12929
FAL: Bodenkarte Kanton Zürich 1 : 5000, Eidgenössische Forschungsanstalt für Agrarökologie und Landbau Zürich, Zürich, 1997. 12913, 12915, 12923, 12942
Franks, S. W., Gineste, P., Beven, K. J., and Merot, P.: On constraining the predictions of a distributed model: the incorporation of fuzzy estimates of saturated areas into the calibration process, Water Resour. Res., 34, 787–797, 1998. 12909, 12911, 12930
Franzmeier, D. P., Yahner, J. E., Steinhardt, G. C., and Sinclair, H. R.: Color patterns and water-table levels in some indiana soils, Soil Sci. Soc. Am. J., 47, 1196–1202, 1983. 12910, 12911
Freer, J. E., McMillan, H., McDonnell, J. J., and Beven, K. J.: Constraining dynamic TOPMODEL responses for imprecise water table information using fuzzy rule based performance measures, J. Hydrol., 291, 254–277, 2004. 12909
Frey, M. P., Schneider, M. K., Dietzel, A., Reichert, P., and Stamm, C.: Predicting critical source areas for diffuse herbicide losses to surface waters: role of connectivity and boundary conditions, J. Hydrol., 365, 23–36, 2009. 12907, 12912
Frey, M. P., Stamm, C., Schneider, M. K., and Reichert, P.: Using discharge data to reduce structural deficits in a hydrological model with a Bayesian inference approach and the

HESSD
10, 12905–12950, 2013

implications for the prediction of critical source areas, Water Resour. Res., 47, W12529, doi:10.1029/2010WR009993, 2011. 12910
Gallart, F., Latron, J., Llorens, P., and Beven, K.: Using internal catchment information to reduce the uncertainty of discharge and baseflow predictions, Adv. Water Resour., 30, 808–823, 2007. 12909
Gemeinde Ossingen: Drainagenkarte 1 : 1000, Flurgenossenschaft Gemeinde Ossingen, Ossingen, 1995. 12913, 12914, 12944
Gemeinde Ossingen: Entwässerungsplan der Gemeinde Ossingen, Gemeinde Ossingen, Ossingen, 2008. 12913, 12914
Gerits, J. J. P., de Lima, J. L. M. P., and van den Broek, T. M. W.: Overland flow and erosion, in: Process Studies in Hillsope Hydrology, edited by: Anderson, M. G. and Burt, T. P., Wiley, Chichester, 173–214, 1990. 12909
Gomides Freitas, L., Singer, H., Müller, S. R., Schwarzenbach, R. P., and Stamm, C.: Source area effects on herbicide losses to surface waters – a case study in the Swiss Plateau, Agr. Ecosyst. Environ., 128, 177–184, 2008. 12908
Grabs, T., Seibert, J., Bishop, K., and Laudon, H.: Modeling spatial patterns of saturated areas: a comparison of the topographic wetness index and a dynamic distributed model, J. Hydrol., 373, 15–23, 2009. 12916
Grayson, R. B., Moore, I. D., and McMahon, T. A.: Physically based hydrologic modeling 1. a terrain-based model for investigative purposes, Water Resour. Res., 26, 2639–2658, 1992a. 12909
Grayson, R. B., Moore, I. D., and McMahon, T. A.: Physically based hydrologic modeling 2. is the concept realistic?, Water Resour. Res., 26, 2659–2666, 1992b. 12909
Güntner, A., Seibert, J., and Uhlenbrook, S.: Modeling spatial patterns of saturated areas: an evaluation of different terrain indices, Water Resour. Res., 40, W05114, doi:10.1029/2003WR002864, 2004. 12910, 12911
Hayes, W. A. and Vepraskas, M. J.: Morphological changes in soils produced when hydrology is altered by ditching, Soil Sci. Soc. Am. J., 64, 1893–1904, 2000. 12911, 12929
Heathwaite, A. L., Quinn, P. F., and Hewett, C. J. M.: Modelling and managing critical source areas of diffuse pollution from agricultural land using flow connectivity simulation, J. Hydrol., 304, 446–461, 2005. 12907, 12908

HESSD
10, 12905–12950, 2013

Hindmarsh, A. C.: A systematized collection of ODE solvers, in: IMACS Transactions on Scientific Computation, edited by: Stepleman, R. S., Scientific Computing, Amsterdam, 55–64, 1983. 12923

Hrachowitz, M., Savenije, H. H. G., Blöschl, G., McDonnell, J. J., Sivapalan, M., Pomeroy, J. W., Arheimer, B., Blume, T., Clark, M. P., Ehret, U., Fenicia, F., Freer, J. E., Gelfan, A., Gupta, H. V., Hughes, D. A., Hut, R. W., Montanari, A., Pande, S., Tetzlaff, D., Troch, P. A., Uhlenbrook, S., Wagener, T., Winsemius, H. C., Woods, R. A., Zehe, E., and Cudennec, C.: A decade of Predictions in Ungauged Basins (PUB) – a review, Hydrolog. Sci. J., 58, 1198–1255, 2013. 12909

Jacobs, P. M., West, L. T., and Shaw, J. N.: Redoximorphic features as indicators of seasonal saturation, Lowndes County, Georgia, Soil Sci. Soc. Am. J., 66, 315–323, 2002. 12910, 12911

Kennedy, J. and Eberhart, R.: Particle swarm optimization, in: Proceedings of the International Conference on Neural Networks (IEEE), vol. 4, Perth, Australia, 1942–1948, doi:10.1109/ICNN.1995.488968, 1995. 12924

Lamb, R., Beven, K., and Myrabø, S.: Use of spatially distributed water table observations to constrain uncertainty in a rainfall–runoff model, Adv. Water Resour., 22, 305–317, 1998. 12909

Leu, C., Singer, H., Stamm, C., Müller, S. R., and Schwarzenbach, R. P.: Simultaneous assessment of sources, processes, and factors influencing herbicide losses to surface waters in a small agricultural catchment, Environ. Sci. Technol., 38, 3827–3834, 2004a. 12907, 12909

Leu, C., Singer, H., Stamm, C., Müller, S. R., and Schwarzenbach, R. P.: Variability of herbicide losses from 13 fields to surface water within a small catchment after a controlled herbicide application, Environ. Sci. Technol., 38, 3835–3841, 2004b. 12908

Leu, C., Singer, H., Müller, S. R., Schwarzenbach, R. P., and Stamm, C.: Comparison of atrazine losses in three small headwater catchments, J. Environ. Qual., 34, 1873–1882, 2005.

Leu, C., Schneider, M. K., and Stamm, C.: Estimating catchment vulnerability to diffuse herbicide losses from hydrograph statistics, J. Environ. Qual., 39, 1441–1450, 2010. 12908

Liess, M. and Schulz, R.: Linking insecticide contamination and population response in an agricultural stream, Environ. Toxicol. Chem., 18, 1948–1955, 1999. 12907

Louchart, X., Voltz, M., Andrieux, P., and Moussa, R.: Herbicide transport to surface waters at field and watershed scales in a Mediterranean vineyard area, J. Environ. Qual., 30, 982–991, 2001. 12908

HESSD
10, 12905–12950, 2013

Lyon, S. W., McHale, M. R., Walter, M. T., and Steenhuis, T. S.: The impact of runoff generation mechanisms on the location of critical source areas, J. Am. Water Resour. As., 42, 793–804, 2006. 12907, 12908, 12909

Maréchal, D. and Holman, I. P.: Development and application of a soil classification-based conceptual catchment-scale hydrological model, J. Hydrol., 312, 277–293, 2005. 12910

Montagne, D., Cornu, S., Le Forestier, L., and Cousin, I.: Soil drainage as an active agent of recent soil evolution: a review, Pedosphere, 19, 1–13, 2009. 12911

Morgan, C. P. and Stolt, M. H.: Soil morphology–water table cumulative duration relationships in southern New England, Soil Sci. Soc. Am. J., 70, 816–824, 2006. 12910, 12911

Nash, J. E. and Sutcliffe, J. V.: River flow forcasting through conceptual models – Part 1: A discussion of principles, J. Hydrol., 10, 282–290, 1970. 12927

Nelder, J. A. and Mead, R.: A simplex method for function minimization, Comput. J., 7, 308–313, 1965. 12925

Petzold, L.: Automatic selection of methods for solving stiff and nonstiff systems of ordinary differential equations, SIAM J. Sci. Stat. Comp., 4, 136–148, 1983. 12923

Pickering, E. W. and Veneman, P. L. M.: Moisture regimes and morphological-characteristics in a hydrosequence in Central Massachusetts, Soil Sci. Soc. Am. J., 48, 113–118, 1984. 12929

Pionke, H. B., Gburek, W. J., Sharpley, A. N., and Schnabel, R. R.: Flow and nutrient export patterns for an agricultural hill–land watershed, Water Resour. Res., 32, 1795–1804, 1996. 12908

Rabiet, M., Margoum, C., Gouy, V., Carluer, N., and Coquery, M.: Assessing pesticide concentrations and fluxes in the stream of a small vineyard catchment – effect of sampling frequency, Environ. Pollut., 158, 737–748, 2010. 12907

Refsgaard, J. C., Storm, B., and Clausen, T.: Système Hydrologique Européen (SHE): review and perspectives after 30 years development in distributed physically-based hydrological modelling, Hydrol. Res., 41, 355–377, 2010. 12909

Schneider, M. K., Brunner, F., Hollis, J. M., and Stamm, C.: Towards a hydrological classification of European soils: preliminary test of its predictive power for the base flow index using river discharge data, Hydrol. Earth Syst. Sci., 11, 1501–1513, doi:10.5194/hess-11-1501-2007, 2007. 12910

Seibert, J., Rodhe, A., and Bishop, K.: Simulating interactions between saturated and unsaturated storage in a conceptual runoff model, Hydrol. Process., 17, 379–390, 2003. 12932

HESSD

10, 12905–12950, 2013

Simonson, G. H. and Boersma, L.: Soil morphology and water table relations: 2. correlation between annual water table fluctuations and profile features, Soil Sci. Soc. Am. Pro., 36, 649–653, 1972. 12910
Srinivasan, M. S. and McDowell, R. W.: Identifying critical source areas for water quality: 1. mapping and validating transport areas in three headwater catchments in Otago, New Zealand, J. Hydrol., 379, 54–67, 2009. 12907, 12908, 12910, 12934
swisstopo: DTM ©2003, reproduced with permission of swisstopo, JA100119, Wabern, Switzerland, 2003. 12913, 12914, 12915
swisstopo: Geologischer Atlas der Schweiz ©2007, reproduced with permission of swisstopo, Wabern, JA100119, Switzerland, 2007. 12913
swisstopo: Vector25 ©2008, reproduced with permission of swisstopo, JA100119, Wabern, Switzerland, 2008. 12942, 12944
Terribile, F., Coppola, A., Langella, G., Martina, M., and Basile, A.: Potential and limitations of using soil mapping information to understand landscape hydrology, Hydrol. Earth Syst. Sci., 15, 3895–3933, doi:10.5194/hess-15-3895-2011, 2011. 12910, 12911
Thurman, E. M., Goolsby, D. A., Meyer, M. T., and Kolpin, D. W.: Herbicides in surface waters of the Midwestern United-States – the effect of spring flush, Environ. Sci. Technol., 25, 1794–1796, 1991. 12907
Vepraskas, M. J. and Wilding, L. P.: Aquic moisture regimes in soils with and without low chroma colors, Soil Sci. Soc. Am. J., 47, 280–285, 1983. 12911
Weiler, M. and McDonnell, J.: Virtual experiments: a new approach for improving process conceptualization in hillslope hydrology, J. Hydrol., 285, 3–18, 2004. 12916, 12917
Wittmer, I. K.: Influence of agricultural pesticide and urban biocide use on load dynamics in surface waters, Ph.D. thesis, Swiss Federal Institute of Technology, Zürich (ETH), 2010. 12921
Wittmer, I. K., Bader, H. P., Scheidegger, R., Singer, H., Lück, A., Hanke, I., Carlsson, C., and Stamm, C.: Significance of urban and agricultural land use for biocide and pesticide dynamics in surface waters, Water Resour. Res., 44, 2850–2862, 2010. 12907

HESSD
10, 12905–12950, 2013

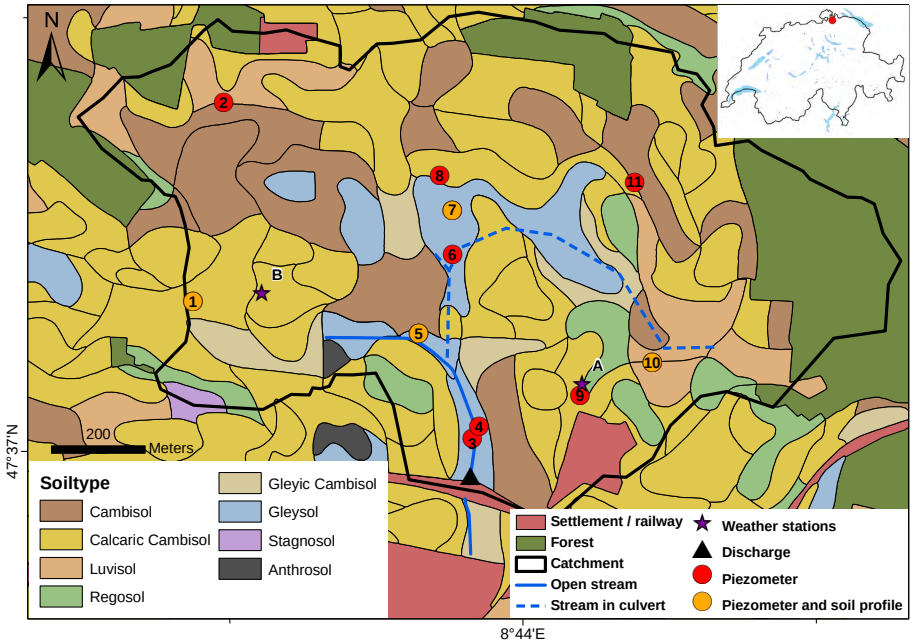

Fig. 1. The experimental catchment with land use, soil types and the hydrological measurement locations. The small map in the top right corner depicts the location of the study site within Switzerland. Sources: swisstopo (2008); FAL (1997).

HESSD
10, 12905–12950, 2013

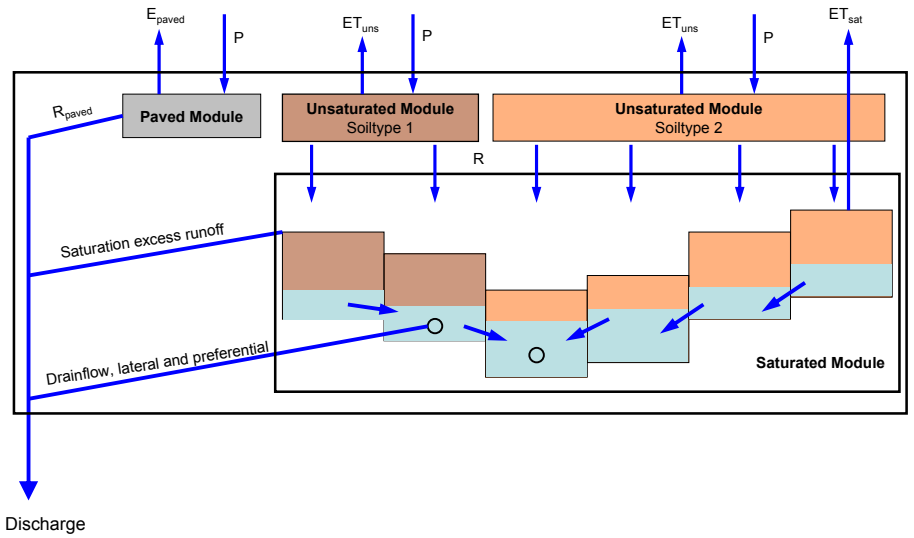

Fig. 2. The model concept, see text.

HESSD
10, 12905–12950, 2013

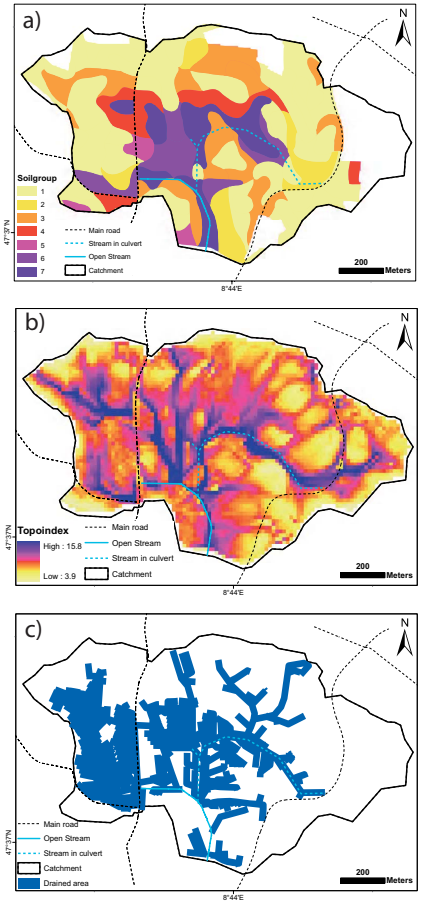

Fig. 3. (a) The reclassified soil map with the seven soil water regime classes (class 1 is the driest, class 7 the wettest), **(b)** map of the topographic wetness index, **(c)** map of the drained areas in the catchment. Sources: Gemeinde Ossingen (1995); swisstopo (2008).

HESSD
10, 12905–12950, 2013

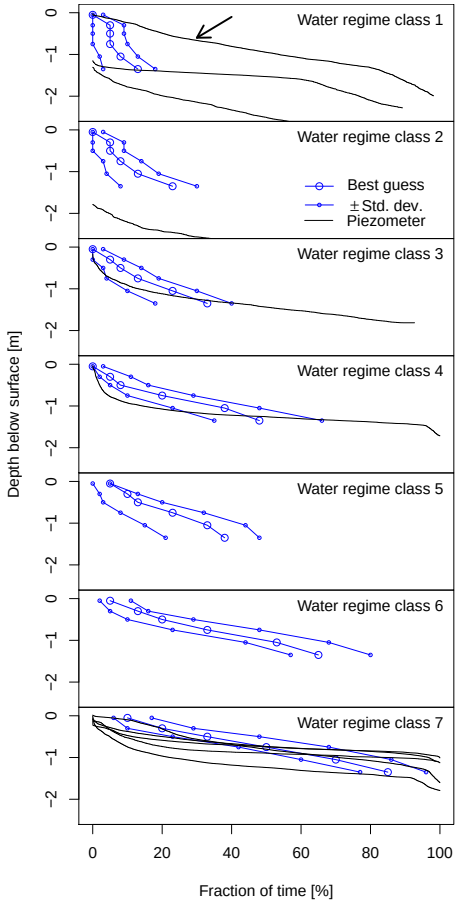

Fig. 4. The estimated depth dependent saturation durations in the seven water regime classes with the expected variation within each class (blue) together with the measured saturation duration in the piezometers (black).

HESSD
10, 12905–12950, 2013

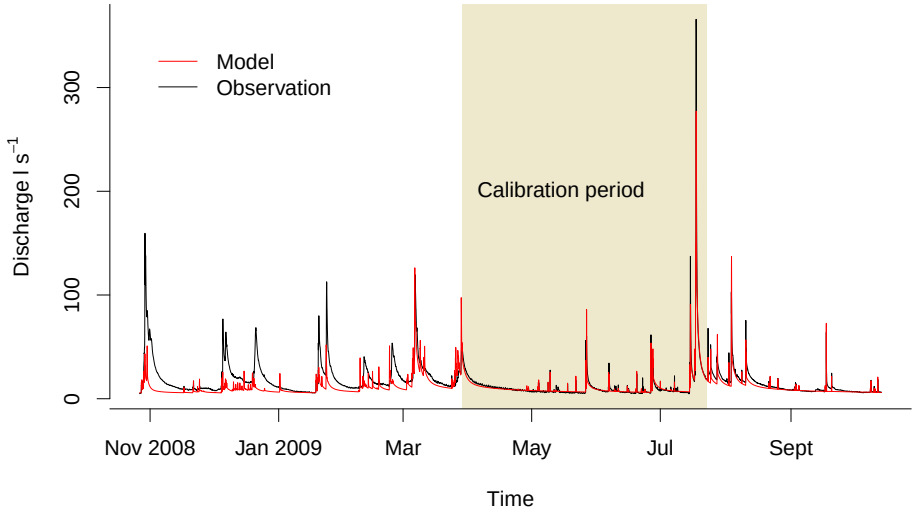

Fig. 5. The modeled and measured discharge time series.

HESSD
10, 12905–12950, 2013

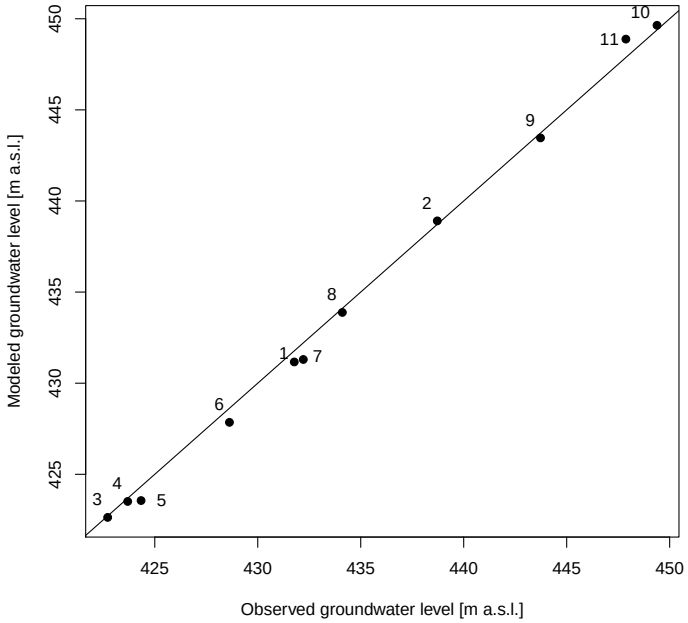

Fig. 6. The observed average groundwater levels plotted against the modeled average groundwater levels at the piezometer locations together with the 1 : 1 line. The numbers indicate the piezometer location (see Fig. 1).

HESSD
10, 12905–12950, 2013

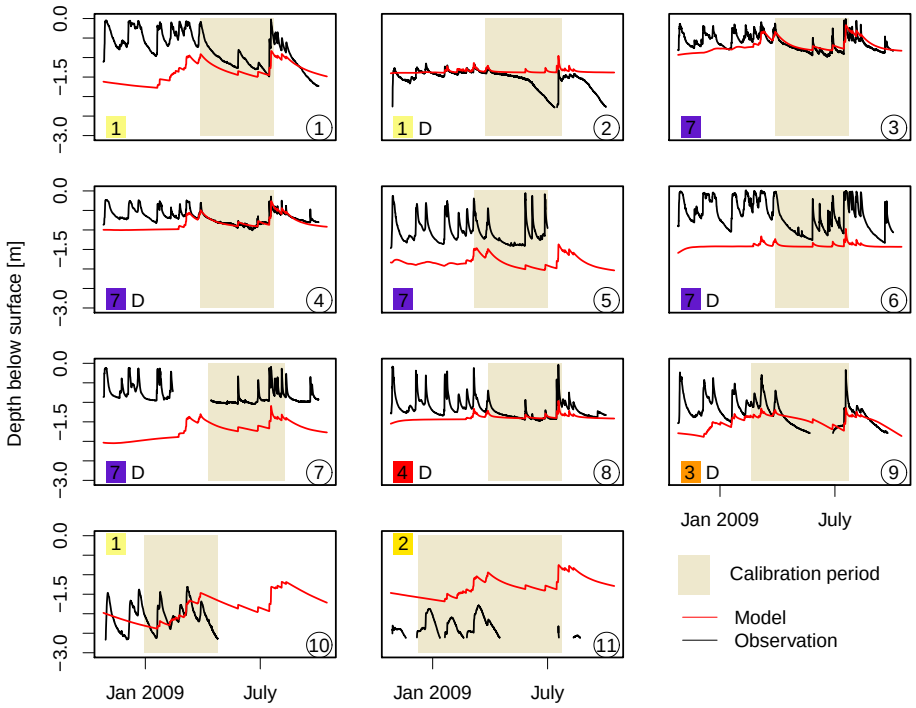

Fig. 7. The modeled and measured groundwater levels at the piezometer locations as depth from the surface. The individual calibration periods are indicated (see Sect. 2.5.4). The circled number is the piezometer location (Fig. 1), the number in the colored box shows the water regime class, D indicates a drained model cell.

HESSD
10, 12905–12950, 2013

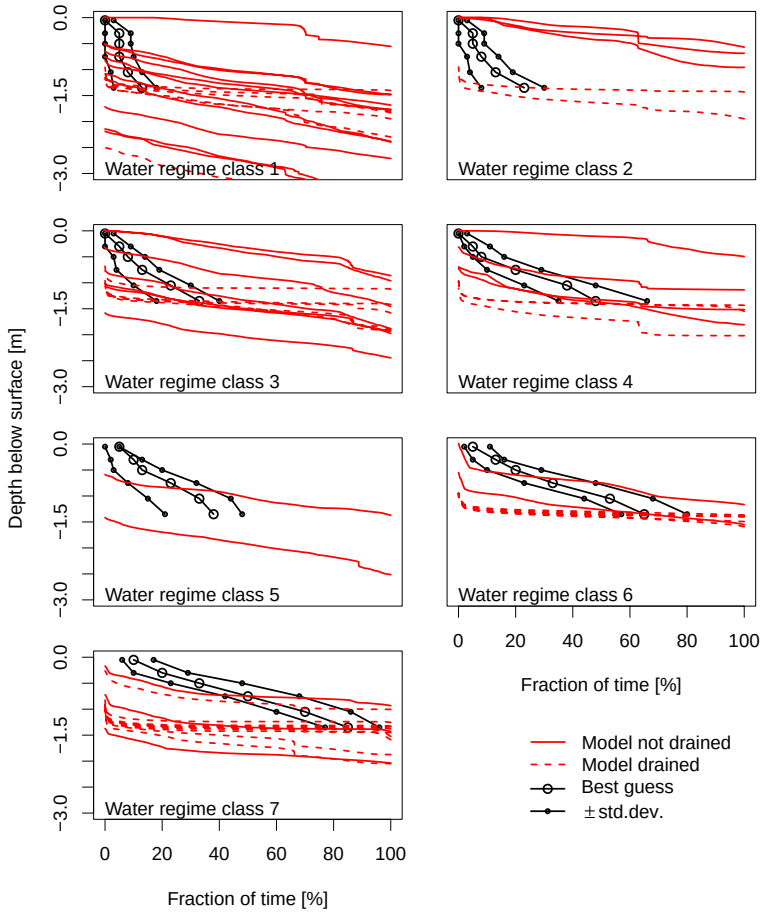

Fig. 8. Comparison of the depth distribution of the saturation duration in selected model cells with the estimate from soil morphology. The model results are grouped into the respective water regime class and into drained and not drained cells.

HESSD
10, 12905–12950, 2013

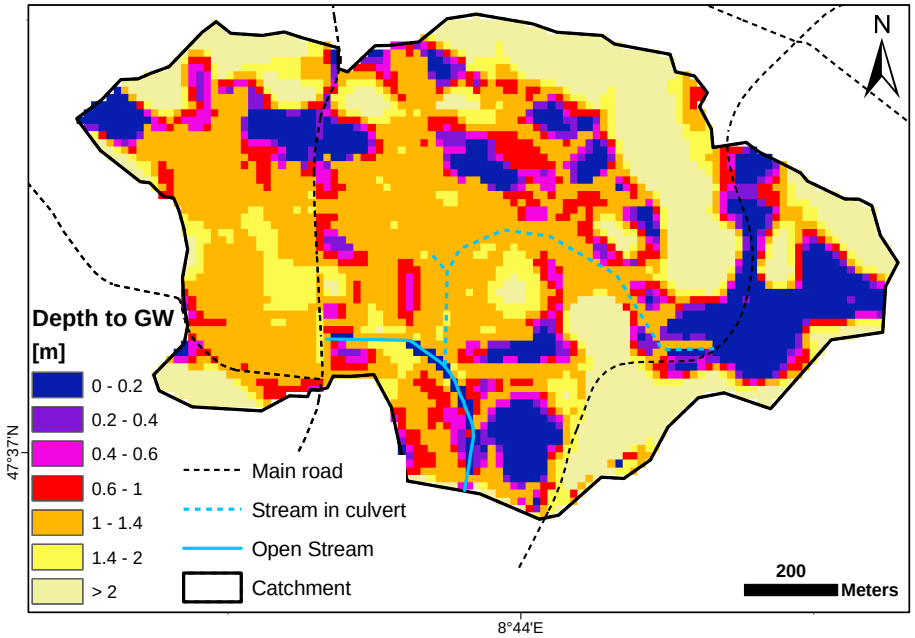

Fig. 9. Map of the modeled depth to groundwater on 27 July 2009.

HESSD
10, 12905–12950, 2013